INTERNATIONAL JOURNAL OF
NUMERICAL ANALYSIS AND MODELING
Volume 11, Number 2, Pages 288–302

A SUBGRID VISCOSITY LAGRANGE-GALERKIN METHOD FOR CONVECTION-DIFFUSION PROBLEMS

RODOLFO BERMEJO, PEDRO GALÁN DEL SASTRE, AND LAURA SAAVEDRA

(Communicated by R. Celorrio)

This paper is dedicated to Francisco Lisbona on occasion of his 65th birthday

Abstract. We present and analyze a subgrid viscosity Lagrange-Galerkin method that combines the subgrid eddy viscosity method proposed in W. Layton, A connection between subgrid scale eddy viscosity and mixed methods. Appl. Math. Comp., 133: 147-157, 2002, and a conventional Lagrange-Galerkin method in the framework of $P_1 \oplus$ cubic bubble finite elements. This results in an efficient and easy to implement stabilized method for convection dominated convection-diffusion-reaction problems. Numerical experiments support the numerical analysis results and show that the new method is more accurate than the conventional Lagrange-Galerkin one.

Key words. Subgrid viscosity, Lagrange-Galerkin, finite elements, convection-diffusion-reaction problems.

1. Introduction

The design of efficient and accurate convection-diffusion algorithms is of significant importance in the computational fluid dynamics community, in particular, when the transport terms of the equations describing the mathematical model become dominant with respect to the diffusion ones. In this case there appear a large variety of spatial-temporal scales that have to be properly resolved in order to obtain a numerical solution sufficiently close to the exact one. The prototype problem to test a convection-diffusion algorithm considers a passive substance, the concentration of which is denoted by $c\,(x,t)$, in a bounded domain $D \subset \mathbb{R}^d$ $(d = 1, 2, 3)$ with Lipschitz continuous boundary ∂D, such that

$$(1) \qquad \begin{cases} \dfrac{\partial c}{\partial t} + \mathbf{b} \cdot \nabla c - \varepsilon \Delta c + \alpha c = f \ \text{ in } D \quad \times (0,T)\,, \\ \\ c = 0 \ \text{ on } \ \partial D \ \times [0,T] \text{ and } \ c(x,0) = v \ \text{ in } \ D, \end{cases}$$

where $\mathbf{b}$ is the velocity vector that for simplicity we shall assume that vanishes on $\partial D \times [0,T]$, $\varepsilon > 0$ is the diffusion coefficient, and $[0,T]$ denotes the time interval. We assume that $\mathbf{b} \in L^\infty(0,T;W^{1,\infty}(D)^d)$, $f \in L^2(0,T;L^2(D))$, $\alpha \in C([0,T];C(D))$, $v \in H^1(D)$, and $\varepsilon \ll \|\mathbf{b}\|_{L^\infty(D\times(0,T))^d}$; moreover, there exists a positive constant $\underline{\alpha}$ such that for all $(x,t) \in D \times [0,t])$, $\alpha(x,t) \geq \underline{\alpha} \geq 0$. In many places the material derivative $\frac{Dc}{Dt} := \frac{\partial c}{\partial t} + \mathbf{b} \cdot \nabla c$ is used.

The dimensionless form of this equation contains the so-called Péclet number Pe defined as $Pe = \frac{UL}{\varepsilon}$, where U and L represent a characteristic velocity and a characteristic length scale respectively. The numerical treatment of this problem is difficult when Pe is large enough because the diffusion term, $\varepsilon\Delta c$, may be considered as a perturbation to the convective term, $\frac{\partial c}{\partial t} + \mathbf{b} \cdot \nabla c$, in regions where $c\,(x,t)$ is smooth so that in these regions the dynamics of the solution is mainly governed

Received by the editors October 29, 2012 and, in revised form, April 8, 2013.
2000 *Mathematics Subject Classification.* 65M12, 65M25, 65M60.

by $\frac{\partial c}{\partial t}+\mathbf{b}\cdot\nabla c$, the latter mathematical expression represents the change of c along the characteristic curves (or trajectories of the flow particles) of the hyperbolic operator $\frac{\partial}{\partial t}+\mathbf{b}\cdot\nabla$. But the existence of boundary conditions to be satisfied by $c\,(x,t)$ on $\partial D\times(0,T)$ is incompatible with the hyperbolic character of $\frac{\partial c}{\partial t}+\mathbf{b}\cdot\nabla c$; hence, the imposition of the boundary conditions will lead to the appearance of a region near the boundary where the solution has to accommodate to satisfy the boundary conditions. This region is termed boundary layer, and one can show through perturbation analysis that its width is $O(Pe^{-\alpha})$, $0<\alpha<1$. Therefore, for high Péclet numbers the boundary layer is narrow and, consequently, the solution will develop a strong gradient in it. It is well known, see for instance [21], that numerical methods based on Galerkin projection (either finite elements, or spectral methods, or hp finite elements) have serious drawbacks in solving the convection-diffusion equation at high Pe numbers for the following reasons: (1) they will develop spurious oscillations (Gibbs phenomenon), which pollute the numerical solution, unless the boundary layers are properly resolved; this means that one has to allocate many mesh-points in regions close to the boundary layers to suppress the spurious oscillations; (2) the error of standard Galerkin methods is of the form

$$\max_{t_n}\|c(t_n)-c_h^n\|_{L^2(D)}=C_G\left(h^m+\Delta t^q\right),$$

where h is the mesh size, Δt the size of the time step, m and q positive real numbers, and the constant C_G is of the form

$$C_G\sim Pe\exp(t_n\max_{D\times[0,t_n]}|\mathbf{b}|\,Pe).$$

Issue (1) and numerical stability reasons require the use of implicit time stepping schemes to advance in time the numerical solution and, consequently, the use of non-symmetric solvers; the latter being less efficient than solvers for symmetric systems.

Following different approaches, such as Eulerian, Eulerian-Lagrangian, and Lagrangian, several algorithms have been devised in the framework of Galerkin methods to overcome the drawbacks described above. In the Eulerian approach one calculates mesh-point values of c at time instants t_n, formulating the numerical method in a fixed mesh with the purpose of suppressing the wiggles without damaging the accuracy of the method. To this respect, we shall refer to the SUPG (Stream-Upwind-Petrov-Galerkin) and the Galerkin/least squares algorithms developed by Hughes and coworkers [6], [17] for convection-diffusion problems of a passive substance, as well as for the Navier-Stokes equations and conservation laws; the edge stabilization methods [7]; the subgrid viscosity methods of [11] and [20], and finally the variational multiscale methods introduced by [16] and further developed by many people.

In the Lagrangian approach one attempts to devise a stable numerical method by allowing the mesh-points to follow the trajectories of the flow. The problem now is that the mesh undergoes large deformations after a number of time steps, due to stretching and shearing, consequently some sort of remeshing has to be done in order to proceed with the calculations. The latter may become a source of large errors.

In the Eulerian-Lagrangian approach the purpose is to get a method that combines the good properties of both the Eulerian and Lagrangian approaches. There have been various methods trying to do so, among them we shall cite the characteristics streamline diffusion (CSD) method, the Eulerian-Lagrangian localized adjoint method (ELLAM), and the Lagrange-Galerkin (LG) methods (also termed Characteristics Galerkin). The CSD method, developed by [12], [13] and [18], combines the good properties of both the Lagrangian methods and the streamline diffusion method by orienting the space-time mesh along the characteristics in space-time, yielding thus to a particular version of the streamline diffusion method. ELLAM was introduced by Celia et al. [8] to calculate a numerical solution for the conservative formulation of (1) by approximating the corresponding adjoint problem, locally in time, with space-time dependent test functions $w(x,t)$ that satisfy the equation, $w_t + \mathbf{b}\cdot\nabla w = 0$, see [26]. The Lagrange-Galerkin methods approximate the material derivative, $\frac{Dc}{Dt}$, at each time step by a backward in time discretization along the characteristics trajectories $X(x,t_{n+1};t)$ of the operator $\frac{\partial}{\partial t} + \mathbf{b}\cdot\nabla$, $t_{n-l} \le t < t_{n+1}$, l being an integer that usually takes the values 0 or 1, with the condition that at $t = t_{n+1}$, $X(x,t_{n+1};t_{n+1}) = x \in D$. The diffusion terms are implicitly discretized in the fixed mesh generated in D. The point here is how to evaluate $c(X(x,t_{n+1};t),t)$. One way to do so is by L^2 projection onto the finite dimensional space associated with the fixed mesh, as the Lagrange-Galerkin methods do, see [1], [5], [23], [9] and [25] just to cite a few; another way is by polynomial interpolation of order higher than one as [4] and [10] propose. When the evaluation of $c(X(x,t_{n+1};t),t)$ is done by polynomial interpolation the method is called semi-Lagrangian.

The assets of LG methods are various: (1) they allow a large time step without damaging the accuracy of the solution; (2) unlike the pure Lagrangian methods, they do not suffer from mesh-deformation so that no remeshing is needed; (3) they yield algebraic symmetric systems of equations to be solved; (4) it can be shown [3] that the constant C in the error estimates of the LG methods is much smaller than the corresponding constant of the standard Galerkin methods and, what it is more important, is uniformly bounded with respect to the values of ε ; however, this does not mean that LG methods are free from the Gibbs phenomenon if the grid is coarse, but such a phenomenon is under control and so is its pollutant effect.

An important drawback of LG methods is the calculation of some integrals whose integrands are the product of functions defined in two different meshes. At high Péclet numbers, and for time steps Δt sufficiently small, such calculations need many quadrature points for the method to be stable, see [22], so they may be computationally expensive. A remedy for this, proposed in this paper, consists of combining LG methods with the subgrid viscosity method of [20]; the subgrid viscosity will act as a stabilizing mechanism killing the instability which appears when the number of quadrature points is not large enough.

2. The numerical method

Let $X := H_0^1(D)$, the weak solution to problem (1) is a function $c : [0,T] \to X$ such that for all $v \in X$

$$\left(\frac{Dc}{Dt}, v\right) + \varepsilon(\nabla c, \nabla v) + (\alpha c, v) = (f, v). \tag{2}$$

To guarantee the existence and uniqueness of the weak solution we also assume that there is a real number $\beta > 0$ such that

$$\alpha - \frac{1}{2} div\ \mathbf{b} \ge \beta. \tag{3}$$

Next, we consider two regular quasi-uniform partitions D_h and D_H of D formed by simplices, and the finite element spaces $X_h \subset X$ and $X_H \subset X$ associated with D_h

and D_H respectively; X_h and X_H are spaces of piecewise polynomials of degrees $m(h)$ and $m(H)$ respectively. Furthermore, we also consider the finite dimensional space of vector-valued functions, $\mathbf{L}_H = \nabla X_H$. The spaces X_h and X_H have the following approximation properties:

(P1) Let $\mu = h, H$. For $v \in H^{r+1}(D) \cap H_0^1(D),\ 1 \le r \le m$,

$$\inf_{u_\mu \in X_\mu} \{\|v - u_\mu\| + \mu \|\nabla(v - u_\mu)\|\} \le C\mu^{r+1} \|v\|_{r+1}\,,$$

where m denotes the degree of the polynomials of X_h and X_H; m may not be the same for X_h and X_H.

(P2)(Inverse inequality) For all $v_\mu \in X_\mu$,

$$\|\nabla v_\mu\| \le C_{inv}\mu^{-1} \|v_\mu\|\,.$$

In these expressions, $\|\bullet\|$ and $\|\bullet\|_r,\ r \ge 1$, are shorthand notations for the norms of the spaces $L^2(D)$ and $H^r(D)$ respectively. Sometimes, we shall identify $H^0(D)$ with $L^2(D)$.

We define in $[0, T]$ a uniform partition $\mathcal{P}_{\Delta t} := 0 = t_0 < t_1 < \ldots < t_N = T$ of uniform step Δt such that the numerical solution to problem (2) is a mapping, $c_h : \mathcal{P}_{\Delta t} \to X_h$, satisfying for all n, $0 \le n \le N-1$, the equations

$$(4)\qquad \begin{cases} \dfrac{(c_h^{n+1} - c_h^n \circ X^{n,n+1}, v_h)}{\Delta t} + (\varepsilon + \varepsilon_d)\,(\nabla c_h^{n+1}, \nabla v_h) \\[2ex] +(\alpha c_h^{n+1}, v_h) - \varepsilon_d(\mathbf{g}_H^{n+1}, \nabla v_h) = (f^{n+1}, v_h), \\[2ex] \left(\mathbf{g}_H^{n+1} - \nabla c_h^{n+1}, \mathbf{l}_H\right) = 0 \quad \forall v_h \in X_h \text{ and } \forall \mathbf{l}_H \in \mathbf{L}_H, \end{cases}$$

where $\mathbf{g}_H^{n+1}$ and f^{n+1} denote the functions $\mathbf{g}_H(\cdot, t_{n+1}) \in \mathbf{L}_H$ and $f(\cdot, t_{n+1})$ respectively, the parameter $\varepsilon_d > 0$ depends on h, and $X^{n,n+1}(x)$, which is a shorthand notation for $X(x, t_{n+1}; t_n)$, denotes the position at time t_n of a particle that at time t_{n+1} will reach the point x; specifically, for $s, t \in [t_n, t_{n+1})$ the mappings $X(\cdot, s; t) : D \to D$ can be defined by solving the system of ordinary differential equations

$$(5)\qquad \begin{cases} \dfrac{dX(x, s; t)}{dt} = \mathbf{b}(X(x, s; t), t), \\[2ex] X(x, s; s) = x \quad \forall x \in D. \end{cases}$$

Noting that $\mathbf{g}_H^{n+1}$ is the L^2 orthogonal projection of $\nabla c_h^{n+1} \in \mathbf{L}^2(D)$ onto $\mathbf{L}_H$, that is, $\mathbf{g}_H^{n+1} = P_{\mathbf{L}_H} \nabla c_h^{n+1}$, where $P_{\mathbf{L}_H} : \mathbf{L}^2(D) \to \mathbf{L}_H$ is the orthogonal projector; it is easy to see, by virtue of the orthogonality property of $P_{\mathbf{L}_H}$, that (4) can be written as

$$(6)\qquad \begin{cases} \left(c_h^{n+1}, v_h\right) + \Delta t\varepsilon \left(\nabla c_h^{n+1}, \nabla v_h\right) + \Delta t\varepsilon_d \left(P_{\mathbf{L}_H}^{\perp} \nabla c_h^{n+1}, P_{\mathbf{L}_H}^{\perp} \nabla v_h\right) \\[2ex] +\Delta t(\alpha c_h^{n+1}, v_h) = (c_h^n \circ X^{n,n+1}, v_h) + \Delta t(f^{n+1}, v_h), \end{cases}$$

where $P_{\mathbf{L}_H}^{\perp} = I - P_{\mathbf{L}_H}$, I being the identity operator in $\mathbf{L}^2(D)$.

3. Error analysis

Our concern in this paper is to estimate the error of LG methods when they are stabilized by a subgrid viscosity scheme, therefore to make clearer and shorter the analysis we shall consider the exact solution of (5); nevertheless, the calculation of a solution of (5) by a numerical method will contribute to the error of the subgrid viscosity LG method, but such a contribution can be estimated using the methodology of [2].

To perform the error analysis of the method we need some preliminary results which are formulated in the following lemmas. The first lemma establishes some properties of the solution of (5) that are well known in the theory of ODE equations [14].

Lemma 1. *Assume that* $\mathbf{b} \in L^{\infty}\ (0,T;W^{k,\infty}(D)^d)$, $k \geq 1$. *Then for any* n, $0 \leq n \leq N-1$, *there exists a unique solution* $t \rightarrow X(x,t_{n+1};t)$ *of (5) such that* $X(x,t_{n+1};\cdot) \in W^{1,\infty}(t_n,t_{n+1};W^{k,\infty}(D)^d)$. *Furthermore, let the multi-index* $\alpha \in \mathbb{N}^d$, *then for all* α, *such that* $1 \leq\mid \alpha \mid\leq k$, $\partial_x^{\alpha} X_i(x,t_{n+1},\cdot) \in C^0([0,T];L^{\infty}(D \times [0,T]))$, $1 \leq i \leq d$.

Lemma 2. *Suppose the assumptions of Lemma 1 hold. For* $|s-t|$ *sufficiently small,* $x \rightarrow X(x,s;t)$ *defines a quasi-isometric map of class* $C^{k-1,1}$ *of* D *onto* D *with Jacobian determinant* $J(x,s;t) \in C([0,T];L^{\infty}(D \times [0,T]))$ *satisfying*

$$\exp(-C_{\mathbf{b}}\,|s-t|) \leq J(x,s;t) \leq \exp(C_{\mathbf{b}}\,|s-t|),$$

where $C_{\mathbf{b}} = \|div\ \mathbf{b}\|_{L^{\infty}(D\times(0,T))}$.

Moreover,

$$K_{\mathbf{b}}^{-1} \mid x-y \mid\leq\mid X(x,s;t) - X(y,s;t) \mid\leq K_{\mathbf{b}} \mid x-y \mid,$$

where $K_{\mathbf{b}} = \exp(\mid s-t \mid \|\nabla \mathbf{b}\|_{L^{\infty}(0;T,L^{\infty}(D)^d)})$. $\mid a-b \mid$ *denotes the Euclidean distance between the points* $a,\ b \in \mathbb{R}^d$.

For a proof of this lemma see [25]. The next two lemmas are given in [20].

Lemma 3. *Let* P *and* P^1 *be the orthogonal projectors with respect to the* L^2 *inner product* (u,v) *and* H^1 *inner product* $(\nabla u,\nabla v)$, *respectively. Then for any* $w \in X$

$$\nabla P^1_{X_H} w = P_{\nabla X_H} \nabla w. \tag{7}$$

Lemma 4. *Let* $\mathbf{L}_h = \nabla X_H$, *there exists a positive constant* C_{inv} *independent of* h *and* H *such that*

$$\left\|\nabla P^1_{X_H} v_h\right\| \leq \|\nabla P_{X_H} v_h\| \leq C_{inv} H^{-1} \|P_{X_H} v_h\| \leq C_{inv} H^{-1} \|v_h\|\,. \tag{8}$$

Let us now define the time-dependent bilinear form

$$a(u,v;t) = \varepsilon\,(\nabla u,\nabla v) + (\alpha(\cdot,t)u,v) + \varepsilon_d \left(P^{\perp}_{\mathbf{L}_H} \nabla u, P^{\perp}_{\mathbf{L}_H} \nabla v\right) \tag{9}$$

for $u,v \in H^1_0(D)$ and a.e. $0 \leq t \leq T$. It is easy to see that $a(u,v;t)$ is symmetric, continuous and coercive so that for functions $u:[0,T] \rightarrow H^1_0(D)$

$$\||u(t)|\|^2 := a(u,u;t) = \varepsilon \|\nabla u(t)\|^2 + \left\|\sqrt{\alpha} u(t)\right\|^2 + \varepsilon_d \left\|P^{\perp}_{\mathbf{L}_H} \nabla u(t)\right\|^2 \tag{10}$$

is a norm. We will use the following continuous and discrete time dependent norms. Continuous norms:

$$\|u\|_{L^{\infty}(H^r)} \equiv \|u\|_{L^{\infty}(0,T;H^r(D))} = \text{ess }\sup\nolimits_{0\leq t\leq T} \|u(t)\|_r\,,\ r \geq 0,$$

$$\|u_t\|_{L^2(L^2)} \equiv \|u_t\|_{L^2(0,T;L^2(D))} = \left(\int_0^T \left\|\frac{\partial u(t)}{\partial t}\right\|^2\right)^{1/2}.$$

Discrete norms:

$$\|u_t\|_{l^\infty(H^r)} \equiv \|u\|_{l^\infty(0,N;H^r(D))} = max_{0\le n\le N} \|u^n\|_r\,,\ r \ge 0,$$

$$\|u_t\|_{l_2(H^r)} \equiv \|u\|_{l_2(0,N;H^r(D))} = \left(\Delta t \sum \|u^n\|_r^2\right)^{1/2},$$

$$|||u|||_{l_2(0,N)} \equiv \left(\Delta t \sum |||u^n|||^2\right)^{1/2}.$$

We will need the version of the discrete Gronwall inequality formulated in [15] that for completeness is presented in the following lemma.

Lemma 5. *Let $\Delta t, B,$ and a_n, b_n, c_n, γ_n, for integers $n \ge 0$ be nonnegative numbers such that*

$$a_N + \Delta t \sum_{n=0}^{N} b_n \le \Delta t \sum_{n=0}^{N} \gamma_n a_n + \Delta t \sum_{n=0}^{N} c_n + B. \tag{11}$$

Suppose that $\Delta t\gamma_n < 1$ for all n, and set $\sigma_n := \frac{1}{1-\Delta t\gamma_n}$. Then

$$a_N + \Delta t \sum_{n=0}^{N} b_n \le \exp\left(\Delta t \sum_{n=0}^{N} \sigma_n\gamma_n\right)\left(\Delta t \sum_{n=0}^{N} c_n + B\right). \tag{12}$$

If the first term on the right in (11) only extends up to $N-1$, then the estimate (12) holds for all $\Delta t > 0$ with $\sigma_n := 1$.

We introduce the interpolant $\Pi_h : H^{m+1}(D) \cap H_0^1(D) \to X_h$ that is used in the analysis. Setting $\rho = c - \Pi_h c$, there is a positive constant C_{ap} independent of h such that

$$\|\rho\|_r \le C_{ap} h^{m+1-r} \|c\|_{m+1}\,, 0 \le r \le m. \tag{13}$$

Similarly, assuming that $c_t \in H^{m+1}(D) \cap H_0^1(D)$

$$\|\rho_t\|_r \le C_{ap} h^{m+1-r} \|c_t\|_{m+1}\,, 0 \le r \le m. \tag{14}$$

Next,we establish an estimate for the error function $e^n = c^n - c_h^n$ for the following cases: (1) $\varepsilon_d = c_1 h^\sigma < 1$ and $H^2 = c_2\varepsilon_d$, $1 \le \sigma < 2$, c_1 and c_2 being positive constants; and (2) $\varepsilon_d = c_3 h < 1$, c_3 being another positive constant, and $H = h$.

Theorem 6. *Let $c \in L^\infty(0,T; H_0^1(D) \cap H^{m+1}(D))$, $c_t \in L^2(0,T; H_0^1(D) \cap H^{m+1}(D))$, $\dfrac{D^2c}{Dt^2} \in L^2(0,T; L^2(D))$, $0 < \Delta t < \Delta t_0 < 1$, and $0 < h < h_0 < 1$. There exists a constant K independent of Δt, h, and ε such that*

(15)

$$\|e\|_{l^\infty(L^2)} + |||e|||_{l^2(0;N)} \le K(\sqrt{\varepsilon+\varepsilon_d}h^m + \left(\sqrt{\overline{\alpha}}+1\right)h^{m+1} + \sqrt{\varepsilon_d}\left\|P_{\mathbf{L}_H}^{\perp}\nabla c^{n+1}\right\|_{l^2(L^2)}$$

$$+ \min\left(\frac{\Delta t}{\sqrt{\varepsilon_d^p}}, \frac{\|\mathbf{b}\|_{l^\infty(\mathbf{L}^\infty)}\Delta t}{h}, 1\right)\frac{h^{m+1}}{\Delta t} + \Delta t) + \|v - v_h\|,$$

where $p = 1$ when $H^2 = c_2\varepsilon_d$, and $p = 2$ when $H = h$; $\overline{\alpha} = max_{(x,t)\in(D\times[0,T])}\alpha(x,t)$.

Proof. We decompose the error at time instant t_{n+1} as

$$e^{n+1} = (c^{n+1} - \Pi_h c^{n+1}) + (\Pi_h c^{n+1} - c_h^{n+1}) \equiv \rho^{n+1} + \theta_h^{n+1},$$

then the errors $\|e\|_{l^\infty(L^2)}$ and $|||e|||_{l_2(0.N)}$ are estimated by applying the triangle inequality and (13) and (14) to estimate ρ, so we need to estimate θ_h. To do so, we notice that subtracting (6) from (2) and after some simple operational work we obtain

$$\begin{aligned}\left(\theta_h^{n+1}-\overline{\theta}_h^n, v_h\right) &+ \Delta t\varepsilon\left(\nabla\theta_h^{n+1}, \nabla v_h\right)\\ +\Delta t\left(\alpha\theta_h^{n+1}, v_h\right) &+ \Delta t\varepsilon_d\left(P_{\mathbf{L}_H}^{\perp}\nabla\theta_h^{n+1}, P_{\mathbf{L}_H}^{\perp}\nabla v_h\right)\\ = &\quad -\Delta t a(\rho^{n+1}, v_h) - \left(\rho^{n+1}-\overline{\rho}^n, v_h\right)\\ &+\Delta t\left(\frac{c^{n+1}-\overline{c}^n}{\Delta t} - \frac{Dc}{Dt}\mid_{t=t_{n+1}}, v_h\right)\\ &+\Delta t\varepsilon_d(P_{\mathbf{L}_H}^{\perp}\nabla c^{n+1}, P_{\mathbf{L}_H}^{\perp}\nabla v_h),\end{aligned}$$

where $\overline{g}^n := g(X(x,t_{n+1};t_n),t_n)$, $g(\cdot,t_n)$ being a generic function defined in D at time instant t_n. Letting $v_h = \theta_h^{n+1}$, see [3], we find that $(\theta_h^{n+1}-\overline{\theta}_h^n, \theta_h^{n+1}) \leq \frac{1}{2}(\|\theta_h^{n+1}\|^2 - \|\theta_h^n\|^2) - \frac{\Delta t C}{2}\|\theta_h^n\|^2$, where C is a positive constant independent of h and Δt, but dependent on div $\mathbf{b}$; then splitting $\rho^{n+1}-\overline{\rho}^n$ as $(\rho^{n+1}-\rho^n)+(\rho^n-\overline{\rho}^n)$ yields

$$\begin{aligned}&\tfrac{1}{2}\left(\left\|\theta_h^{n+1}\right\|^2 - \|\theta_h^n\|^2\right) + \Delta t\,|||\theta_h^{n+1}|||^2\\ \leq &\quad \Delta t\left|a(\rho^{n+1},\theta_h^{n+1})\right| + \left|\left(z_1^{n+1}, P_{\mathbf{L}_H}^{\perp}\nabla\theta_h^{n+1}\right)\right|\\ &+\frac{C}{2}\Delta t\,\|\theta_h^n\|^2 + \left|\sum_{i=2}^{4}\left(z_i^{n+1},\theta_h^{n+1}\right)\right|,\end{aligned}\tag{16}$$

where

$$\begin{cases} z_1^{n+1} = \Delta t\varepsilon_d P_{\mathbf{L}_H}^{\perp}\nabla c^{n+1}, & z_2^{n+1} = -(\rho^{n+1}-\rho^n),\\ z_3^{n+1} = \Delta t\left(\dfrac{c^{n+1}-\overline{c}^n}{\Delta t} - \dfrac{Dc}{Dt}\mid_{t=t_{n+1}}\right), & z_4^{n+1} = -(\rho^n-\overline{\rho}^n).\end{cases}\tag{17}$$

To estimate $\Delta t\left|a(\rho^{n+1}, v_h)\right|$ we notice that by virtue of Lemma **??** and Young's inequality, $ab \leq \frac{\epsilon}{2}a^2 + \frac{1}{2\epsilon}b^2$, a, b and $\epsilon > 0$ real numbers, it follows that

$$\begin{aligned}\Delta t\left|a(\rho^{n+1},\theta_h^{n+1})\right| &\leq \Delta t\,|||\rho^{n+1}|||\;|||\theta_h^{n+1}|||\\ &\leq \Delta t\left(\tfrac{\alpha_1}{2}|||\rho^{n+1}|||^2 + \tfrac{1}{2\alpha_1}|||\theta_h^{n+1}|||^2\right).\end{aligned}\tag{18}$$

Next, we estimate the terms $\left|\left(z_i^{n+1},\theta_h^{n+1}\right)\right|$.

$$\left|\left(z_1^{n+1}, P_{\mathbf{L}_h}^{\perp}\nabla\theta_h^{n+1}\right)\right| \leq \Delta t\varepsilon_d\left\|P_{\mathbf{L}_H}^{\perp}\nabla c^{n+1}\right\|\left\|P_{\mathbf{L}_H}^{\perp}\nabla\theta_h^{n+1}\right\|.$$

Applying Young's inequality it follows that

$$\left|\left(z_1^{n+1}, P_{\mathbf{L}_H}^{\perp}\nabla\theta_h^{n+1}\right)\right| \leq \frac{\alpha_2\Delta t\varepsilon_d}{2}\left\|P_{\mathbf{L}_H}^{\perp}\nabla c^{n+1}\right\|^2 + \frac{\Delta t}{2\alpha_2}\varepsilon_d\left\|P_{\mathbf{L}_H}^{\perp}\nabla\theta_h^{n+1}\right\|^2.\tag{19}$$

To estimate $\left|\left(z_2,\theta_h^{n+1}\right)\right|$, we note that by virtue of the Cauchy-Schwarz inequality

$$\left|\int_D\left(\int_{t_n}^{t_{n+1}}\rho_t dt\right)\theta_h^{n+1}dx\right| \leq \left\|\int_{t_n}^{t_{n+1}}\rho_t dt\right\|\left\|\theta_h^{n+1}\right\|,$$

and

$$\left\|\int_{t_n}^{t_{n+1}} \rho_t dt\right\|^2 = \int_D \left|\int_{t_n}^{t_{n+1}} \rho_t dt\right|^2 dx \leq \Delta t \left(\int_{t_n}^{t_{n+1}} |\rho_t|^2 \, dt\right) dx;$$

hence,

$$\left\|\int_{t_n}^{t_{n+1}} \rho_t dt\right\| \leq \Delta t^{1/2} \|\rho_t\|_{L^2(t_n,t_{n+1},L^2)},$$

and using the Young's inequality in $\left\|\int_{t_n}^{t_{n+1}} \rho_t dt\right\| \|\theta_h^{n+1}\|$ yields

$$\left|(z_2, \theta_h^{n+1})\right| \leq \left\|\int_{t_n}^{t_{n+1}} \rho_t dt\right\| \|\theta_h^{n+1}\| \leq \frac{\Delta t \zeta}{2} \|\theta_h^{n+1}\|^2 + \frac{1}{2\zeta} \|\rho_t\|^2_{L^2(t_n,t_{n+1},L^2)}, \tag{20}$$

where the positive constant ζ is $O(T^{-1})$ and does not depend on ε. Next, by a Taylor expansion along the curves $X(x, t_{n+1}, t)$ it follows that

$$\|z_3^{n+1}\| = \Delta t \left(\int_D \left|\frac{1}{\Delta t}\int_{t_n}^{t_{n+1}} (t-t_n)\frac{D^2 c}{Dt^2} dt\right|^2 dx\right)^{1/2}$$

$$\leq \frac{\Delta t^{3/2}}{\sqrt{3}} \left\|\frac{D^2 c}{Dt^2}\right\|_{L^2(t_n,t_{n+1};L^2)};$$

then by using both the Cauchy-Schwarz and Young's inequalities it follows that

$$\left|(z_3^{n+1}, \theta_h^{n+1})\right| \leq \frac{1}{6\zeta}\Delta t^2 \left\|\frac{D^2 c}{Dt^2}\right\|^2_{L^2(t_n,t_{n+1};L^2)} + \frac{\Delta t \zeta}{2} \|\theta_h^{n+1}\|^2. \tag{21}$$

To bound the term $\left|(z_4^{n+1}, \theta_h^{n+1})\right|$ we need a lemma the proof of which is given in [3].

Lemma 7. *For all n, $\rho^n - \rho^n \circ X^{n,n+1}$ satisfies the following bounds:*

$$\left\|\rho^n - \rho^n \circ X^{n,n+1}\right\|_{H^{-1}} \leq K_4 \Delta t \|\rho^n\|, \tag{22a}$$

$$\left\|\rho^n - \rho^n \circ X^{n,n+1}\right\| \leq K_5 \Delta t \|\nabla \rho^n\|, \tag{22b}$$

$$\left\|\rho^n - \rho^n \circ X^{n,n+1}\right\| \leq K_6 \|\rho^n\|, \tag{22c}$$

where H^{-1} denotes the dual space of $H_0^1(D)$, and

$$\begin{cases} K_4 = \|\mathbf{b}\|_{L^\infty(\mathbf{L}^\infty)} + C_{ap} K_3 (1 + K_3 \Delta t), \\ K_5 = (1 + K_3 \Delta t) \|\mathbf{b}\|_{L^\infty(\mathbf{L}^\infty)}, \\ K_6 = 1 + (1 + K_3 \Delta t), \end{cases} \tag{23}$$

*K_3 being a positive constant depending on div **b**.*

Based on the results of this lemma we obtain three different estimates for $\left|(z_4^{n+1}, \theta_h^{n+1})\right|$, namely,

$$\begin{aligned} \left|(z_4^{n+1}, \theta_h^{n+1})\right|_{(1)} &\leq \|\rho^n - \overline{\rho}^n\|_{-1} \left\|\nabla\theta_h^{n+1}\right\| \leq K_4 \Delta t \|\rho^n\| \left\|\nabla\theta_h^{n+1}\right\|, \\ \left|(z_4^{n+1}, \theta_h^{n+1})\right|_{(2)} &\leq \|\rho^n - \overline{\rho}^n\| \left\|\theta_h^{n+1}\right\| \leq K_5 \Delta t \|\nabla\rho^n\| \left\|\theta_h^{n+1}\right\|, \\ \left|(z_4^{n+1}, \theta_h^{n+1})\right|_{(3)} &\leq \|\rho^n - \overline{\rho}^n\| \left\|\theta_h^{n+1}\right\| \leq K_6 \Delta t \left\|\frac{\rho^n}{\Delta t}\right\| \left\|\theta_h^{n+1}\right\|. \end{aligned} \tag{24}$$

Estimate for $\left|(z_4^{n+1}, \theta_h^{n+1})\right|_{(1)}$.

Noting that $\nabla\theta_h^{n+1} = P_{\mathbf{L}_H}\nabla\theta_h^{n+1} + P_{\mathbf{L}_H}^{\perp}\nabla\theta_h^{n+1}$ it follows that

$$\left|(z_4^{n+1}, \theta_h^{n+1})\right|_1 \leq \Delta t K_4 \|\rho^n\| \left(\left\|P_{\mathbf{L}_H}\nabla\theta_h^{n+1}\right\| + \left\|P_{\mathbf{L}_H}^{\perp}\nabla\theta_h^{n+1}\right\|\right). \tag{25}$$

We invoke Lemma 4 and Lemma 3 to estimate $\left\|P_{\mathbf{L}_H}\nabla\theta_h^{n+1}\right\| \leq C_{inv} H^{-1} \left\|\theta_H^{n+1}\right\|$; hence, applying Young's inequality in (25) it follows that when $\varepsilon_d = c_3 h^{\sigma}$ and $H = c_2\varepsilon_d$, $1 \leq \sigma < 2$,

$$\left|(z_4^{n+1}, \theta_h^{n+1})\right|_1 \leq \frac{\Delta t K_4^2}{\varepsilon_d} \|\rho^n\|^2 + \frac{\Delta t \varepsilon_d}{4H^2} C_{inv}^2 \left\|\theta_h^{n+1}\right\|^2 + \frac{\Delta t \varepsilon_d}{8} \left\|P_{\mathbf{L}_H}^{\perp}\nabla\theta_h^{n+1}\right\|, \tag{26a}$$

and when $\varepsilon_d = c_3 h$ and $H = h$,

$$\begin{aligned} \left|(z_4^{n+1}, \theta_h^{n+1})\right|_1 &\leq \tfrac{\Delta t K_4^2}{\varepsilon_d^2} \|\rho^n\|^2 + \tfrac{\Delta t \varepsilon_d^2}{4h^2} C_{inv}^2 \left\|\theta_h^{n+1}\right\|^2 + \tfrac{\Delta t \varepsilon_d^2}{8} \left\|P_{\mathbf{L}_H}^{\perp}\nabla\theta_h^{n+1}\right\| \\ &\leq \tfrac{\Delta t K_4^2}{\varepsilon_d^2} \|\rho^n\|^2 + \tfrac{\Delta t \varepsilon_d^2}{4h^2} C_{inv}^2 \left\|\theta_h^{n+1}\right\|^2 + \tfrac{\Delta t \varepsilon_d}{8} \left\|P_{\mathbf{L}_H}^{\perp}\nabla\theta_h^{n+1}\right\|, \end{aligned} \tag{26b}$$

the second inequality on the right is obtained by noting that $\varepsilon_d = c_3 h < 1$. Let $\lambda_1 = \frac{\varepsilon_d C_{inv}^2}{4H^2} = \frac{c_1 C_{inv}^2}{4c_2}$ and $\lambda_2 = \frac{\varepsilon_d^2 C_{inv}^2}{h^2} = \frac{c_3^2 C_{inv}^2}{4}$, setting $\alpha_1 = 2$ and $\alpha_2 = 4$ in (18) and (19) respectively, and substituting the estimates (18)-(21), (26a) or (26b), as it corresponds, on the right hand side of (16) yields

$$\begin{aligned} &\left\|\theta_h^{n+1}\right\|^2 - \|\theta_h^n\|^2 + \frac{\Delta t}{2} \left|\left|\left|\theta_h^{n+1}\right|\right|\right|^2 + \frac{\Delta t}{2}\left(\varepsilon \left\|\nabla\theta_h^{n+1}\right\|^2 + \overline{\alpha} \left\|\theta_h^{n+1}\right\|^2\right) \\ &\leq 2\Delta t \left|\left|\left|\rho^{n+1}\right|\right|\right|^2 + \frac{1}{\zeta} \|\rho_t\|^2_{L^2(t_n, t_{n+1}, L^2(D))} + \frac{6\Delta t K_4^2}{\varepsilon_d^p} \|\rho^n\|^2 \\ &+ \frac{1}{3\zeta}\Delta t^2 \left\|\frac{D^2 c}{Dt^2}\right\|^2_{L^2(t_n, t_{n+1}; L^2(D))} + 4\Delta t \varepsilon_d \left\|P_{\mathbf{L}_H}^{\perp}\nabla c^{n+1}\right\|^2 \\ &+ \Delta t\,(2\zeta + \lambda) \left\|\theta_h^{n+1}\right\|^2 + \Delta t C \|\theta_h^n\|^2, \end{aligned} \tag{27}$$

where $\lambda = \max(\lambda_1, \lambda_2)$, $p = 1$ if $H^2 = c_2\varepsilon_d$, and $p = 2$ if $H = h$. Let $\zeta = O(T^{-1})$, choosing $\Delta t < \Delta t_0$, where Δt_0 is such that $\Delta t_0(2\zeta + \lambda) < 1$, we obtain, adding from $n = 0$ up to $n = N - 1$ and applying the discrete Gronwall inequality, that

$$\|\theta_h\|_{l^\infty(L^2)} + |||\theta_h|||_{l_2(0,N)} \leq K_1 \left(\begin{array}{l} |||\rho|||_{l_2(0,N)} + \|\rho_t\|_{L^2(L^2)} + \sqrt{\varepsilon_d} \left\|P_{\mathbf{L}_H}^{\perp}\nabla c\right\|_{l_2(L^2)} \\ + \frac{K_4}{\sqrt{\varepsilon_d^p}} \|\rho\|_{l_2(L^2)} + \Delta t \left\|\frac{D^2 c}{Dt^2}\right\|_{L^2(L^2)} \end{array}\right). \tag{28}$$

where $K_1 = C_1 \exp(T(\zeta + \lambda))$, and $C_1 = O(T^{1/2})$; we have assumed that $\left\|\theta_h^0\right\| = 0$.

Estimate for $\left|(z_4^{n+1},\theta_h^{n+1})\right|_{(2)}$.

$$\left|(z_4^{n+1},\theta_h^{n+1})\right|_2 \leq \frac{K_5^2\Delta t}{2\zeta}\left\|\nabla\rho^n\right\|^2+\frac{\Delta t\zeta}{2}\left\|\theta_h^{n+1}\right\|^2. \tag{29}$$

Setting $\alpha_1=\alpha_2=2$ in (18) and (19) respectively, and substituting the estimates (18)-(21), and (29) on the right hand side of (16) yields

$$\begin{aligned}&\left\|\theta_h^{n+1}\right\|^2-\left\|\theta_h^n\right\|^2+\Delta t\left|\left|\left|\theta_h^{n+1}\right|\right|\right|^2+\frac{\Delta t}{2}\left(\varepsilon\left\|\nabla\theta_h^{n+1}\right\|^2+\overline{\alpha}\left\|\theta_h^{n+1}\right\|^2\right)\\ &\leq 2\Delta t\left|\left|\left|\rho^{n+1}\right|\right|\right|^2+\frac{1}{\zeta}\left\|\rho_t\right\|^2_{L^2(t_n,t_{n+1},L^2)}+\frac{\Delta t K_5^2}{\zeta}\left\|\nabla\rho^n\right\|^2\\ &+\frac{1}{3\zeta}\Delta t^2\left\|\frac{D^2c}{Dt^2}\right\|^2_{L^2(t_n,t_{n+1};L^2)}+2\Delta t\varepsilon_d\left\|P^\perp_{\mathbf{L}_H}\nabla c^{n+1}\right\|^2\\ &+\Delta t3\zeta\left\|\theta_h^{n+1}\right\|^2+\Delta t C\left\|\theta_h^n\right\|^2.\end{aligned}$$

Letting $\zeta=O(T^{-1})$ and $\Delta t<\Delta_0$, with Δ_0 be such that $3\Delta t_0\zeta<1$, then by adding from $n=0$ up to $n=N-1$, and applying the discrete Gronwall inequality yields another estimate for $\left\|\theta_h^N\right\|+|||\theta_h|||_{l_2(0,N)}$:

(30)

$$\left\|\theta_h^N\right\|+|||\theta_h|||_{l_2(0,N)}\leq K_2\left(\begin{array}{l}|||\rho|||_{l_2(0,T)}+\left\|\rho_t\right\|_{L^2(L^2)}+\sqrt{\varepsilon_d}\left\|P^\perp_{\mathbf{L}_H}\nabla c\right\|_{l_2(L^2)}\\ +K_5\left\|\nabla\rho\right\|_{l_2(L^2)}+\Delta t\left\|\frac{D^2c}{Dt^2}\right\|_{L^2(L^2)}\end{array}\right).$$

where $K_2=C_2\exp(T(3/2\zeta+C))$ and $C_2=O(T^{1/2})$.

Estimate for $\left|(z_4^{n+1},\theta_h^{n+1})\right|_{(3)}$.

$$\left|(z_4^{n+1},\theta_h^{n+1})\right|_3\leq\frac{K_6^2\Delta t}{2\zeta}\left\|\frac{\rho^n}{\Delta t}\right\|^2+\frac{\zeta\Delta t}{2\zeta_2}\left\|\theta_h^{n+1}\right\|^2. \tag{31}$$

Arguing as for the estimate (30), we obtain a new estimate

(32)

$$\left\|\theta_h^N\right\|+|||\theta_h|||_{l_2(0,N)}\leq K_2\left(\begin{array}{l}|||\rho|||_{l_2(0,N)}+\left\|\rho_t\right\|_{L^2(L^2)}+\sqrt{\varepsilon_d}\left\|P^\perp_{\mathbf{L}_H}\nabla c\right\|_{l_2(L^2)}\\ +K_6\left\|\frac{\rho}{\Delta t}\right\|_{l_2(L^2)}+\Delta t\left\|\frac{D^2c}{Dt^2}\right\|_{lL^2(L^2)}\end{array}\right).$$

Considering (23), we substitute the constants K_1K_4 in (28), K_2K_5 in (30), and K_2K_6 in (32) by G, $G\|\mathbf{b}\|_{l^\infty(\mathbf{L}^\infty)}$, and G, respectively, where $G=\max(K_1K_4,K_2(1+K_3\Delta t),K_2K_6)$; then defining $K^*=\max(K_1,K_2,G)$ and using (13) we can recast (28), (30), and (32) all together as

(33)

$$\|\theta_h\|_{l^\infty(L^2)}+|||\theta_h|||_{l_2(0,N)}\leq K^*\left(\begin{array}{l}|||\rho|||_{l_2(0,N)}+\sqrt{\varepsilon_d}\left\|P^\perp_{\mathbf{L}_H}\nabla c\right\|_{l_2(L^2)}\\ +\left\|\rho_t\right\|_{L^2(L^2)}+\Delta t\left\|\frac{D^2c}{Dt^2}\right\|_{L^2(L^2)}\\ +\min\left(\frac{\Delta t}{\sqrt{\varepsilon_d^p}},\frac{\|\mathbf{b}\|_{l^\infty(\mathbf{L}^\infty)}\Delta t}{h},1\right)\frac{h^{m+1}}{\Delta t}C_{ap}\left\|\rho\right\|_{l_2(L^2)}.\end{array}\right).$$

Substituting the estimates for $\|\rho\|_{l_2(L^2)}$, $\|\rho\|_{l_2(H^1)}$, $\|\rho_t\|_{L^2(L^2)}$, see (13) and (14), into (33) we obtain (15). □

4. Numerical results

We present in this section a numerical experiment proposed in [19] to illustrate the behavior of an Eulerian two-level subgrid viscosity method for convection dominated convection-diffusion equations. The differences between the method proposed in [19] and ours are the following: (1) we discretize the material derivative by a first order in time Lagrange-Galerkin method , and (2) we use a one level mesh method via $P_1 \oplus$ bubble elements. Thus, the finite elements spaces, X_h, X_H and $\mathbf{L}_H$ are defined as follows:

$$X_h = \{v_h \in C(\overline{D}) : v_h \mid_T \in P_1(T) \oplus B(T) \ \forall T \in D_h\},$$

$$X_H = \{v_H \in C(\overline{D}) : v_H \mid_T \in P_1(T) \ \forall T \in D_h\},$$

$$\mathbf{L}_H = \nabla X_H = \{\mathbf{w}_H \in L^2(D) \times L^2(D) : \mathbf{w}_H \mid_T \in (P_0(T))^2 \ \forall T \in D_h\},$$

where $P_1(T)$ and $P_0(T)$ are the set of polynomials of degree ≤ 1 and 0, respectively, defined in T, and $B(T)$ is the set of cubic bubbles defined in T that are zero on ∂T. We remark that with this choice of spaces it holds that $\mathbf{L}_H \subset \nabla X_h$. Following [24] we choose an orthogonal L^2 projector $P_{\mathbf{L}_H} : \mathbf{L}^2 \to \mathbf{L}_H$ of the form $P_{\mathbf{L}_H}\mathbf{w}|_T = \mathbf{w}(b)$, where b is the baricenter of the element T. Note that this projector is the result of approximating the integrals of the expression

$$\int_D \mathbf{w} \cdot \mathbf{w}_H dx = \int_D P_{\mathbf{L}_H}\mathbf{w} \cdot \mathbf{w}_H dx \quad \forall \mathbf{w}_H \in \mathbf{L}_H$$

by the one point Gaussian quadrature rule in triangles. This choice of spaces and L^2 projector yields an efficient and easy to implement algorithm for a low order subgrid viscosity method via equation (6), in contrast with two-level subgrid viscosity methods (see [19]) that have to be implemented via the mixed formulation (4) and, therefore, they have to calculate at each time t_n the variables $\mathbf{g}_H^n$ and c_h^n.

Integrals of the form $\int_D c_h^n \circ X^{n,n+1} \phi_i dx$, where ϕ_i is the i-th global basis function of X_h, appear in the first term on the right side of (6); these integrals are typical of LG methods and, in practice, cannot be calculated exactly so that they have to be approximated by a quadrature rule of high order to keep the theoretical stability and accuracy of the method. Let $\{x_g\}$ be the set of quadrature points of the rule employed in the calculations of the integrals of (6), we calculate the points $X^{n,n+1}(x_g)$ by solving (5) with a Runge-Kutta method of order 4 to have the error of such calculations much smaller than the own error of the method given in Theorem 6. In the numerical experiments that follow we have tested the performance of the subgrid viscosity LG method employing Gauss-Legendre quadrature rules of order 5, 10, and 14, which have 7, 25, and 42 quadrature points respectively.

The domain $D := (0,1)^2$, and the triangular meshes D_h are generated from a uniform square mesh of size h by dividing the squares using the diagonals from the left lower corner to the right upper corner. In Table 1 we show the features of the meshes used in the experiments.

The prescribed solution is

$$c(x,t) = t\cos(xy^2),$$

for the parameters of equation (1): $\varepsilon = 10^{-8}$, $\mathbf{b} = (2,-1)$, $\alpha = 1$ and $T = 1$. The non-homogenous Dirichlet boundary conditions and the forcing term f are chosen such that the prescribed solution satisfies (1). In the numerical tests we have used different values of ε_d to test how sensitive is the numerical solution to this parameter.

TABLE 1. Features of the meshes

h	Elements	Vertices	Nodes
1/8	128	81	289
1/16	512	289	1089
1/32	2048	1089	4225
1/64	8192	4225	16641
1/128	32768	16641	66049

We calculate the error

$$Err_1 = |||c - c_h|||_{l_2(0,N)} := \left(\Delta t \sum_{n=0}^{N} \epsilon \| c^n - c_h^n \|_{H^1}^2 \right)^{1/2}. \tag{34}$$

Table 4 and Table 3 show the error for time steps $\Delta t = 0.0002$ and $\Delta t = 0.0001$ respectively for different meshes and values of ε_d. The quadrature rule used in these calculations is of order five. Since the time steps are so small, then the errors represented in these tables can be considered spatial errors.

TABLE 2. Error for different meshes with $\Delta t = 0.0002$

h	$Err_1, \varepsilon_d = 100h^2$	$Err_1, \varepsilon_d = 10h^2$
1/8	3.04E-06	2.84E-06
1/16	1.48E-06	1.37E-06
1/32	6.96E-07	7.12E-07
1/64	3.35E-07	4.12E-07
1/128	1.68E-07	2.64E-07

TABLE 3. Error for different meshes with $\Delta t = 0.0001$

h	$Err_1, \varepsilon_d = 100h$	$Err_1, \varepsilon_d = 10h$	$Err_1, \varepsilon_d = h$
1/8	3.07E-06	3.03E-06	2.79E-06
1/16	1.53E-06	1.50E-06	1.37E-06
1/32	7.60E-07	7.32E-07	6.76E-07
1/64	3.67E-07	3.51E-07	3.36E-07
1/128	1.74E-07	1.69E-07	1.67E-07

From the inspection of these tables we see that the the solution is not very sensitive to the values of ε_d, although the best choice it seems to be $\varepsilon_d = h$, and the worst is $\varepsilon_d = 10h^2$; moreover, the error $|||c - c_h|||_{l_2(0,N)}$ is $O(h)$ for $\varepsilon_d = 100h$, $10h$ and h. The results of Table 3 are in accordance with Theorem 6 because for such values of ε_d the term in Theorem 6 that controls the error is: $\min(\frac{\Delta t}{\sqrt{\varepsilon_d^p}}, \frac{\|\mathbf{b}\|_{l^\infty(\mathbf{L}^\infty)}\Delta t}{h}, 1)\dfrac{h^{m+1}}{\Delta t} = \dfrac{\Delta t}{\sqrt{\varepsilon_d^p}}\dfrac{h^{m+1}}{\Delta t} = O(h)$ where $p = 2$ and $m = 1$.

In the next figures we illustrate the influence of the order of the quadrature rule in the numerical solution; in fact, we want to see how the subgrid viscosity stabilizes the LG method when the integrals $\int_D c_h^n \circ X^{n,n+1} \phi_i dx$ are not calculated exactly. To this end, we represent the variation of the error Err_1 as a function of Δt in the finest mesh $h = 1/128$ for different values of ε_d, namely, $\varepsilon_d = 0$, $\varepsilon_d = 0.0008h$, $\varepsilon_d = 0.08h$

and $\varepsilon_d = 0.8h$, and with quadrature rules of order five, ten and fourteen. Two remarks are in order. (1) The error curves calculated with $\varepsilon_d = 0$, $\varepsilon_d = 0.0008h$, $\varepsilon_d = 0.08h$ and $\varepsilon_d = 0.8h$ are denoted in Figures 1 and 2 as LG+P1b; LG+P1b, $\varepsilon_d = 0.1h^2$; LG+P1b, $\varepsilon_d = 10h^2$; and LG+P1b, $\varepsilon_d = 100h^2$ respectively. (2) The quadrature rule of order 5 does not calculate exactly neither the coefficients of the mass matrix, i.e., $\int_D \phi_i\phi_j dx$, nor the integrals on the right side of (6) when $P_1\oplus$ cubic bubble elements are used; to calculate exactly the coefficients of the mass matrix when these elements are employed the quadratures rules should be of order larger than or equal to 6.

We note in Figure 1 that the conventional LG method and the subgrid viscosity LG method with $\varepsilon_d = 0.0008h$ become unstable for Δt sufficiently small, this means that this value of the artificial diffusion is not strong enough to kill the instabilities that appear at low CFL numbers due to the error in the calculation of the integrals on the right side of (6); however, by increasing the artificial diffusion the LG method becomes more stable and accurate as occurs with $\varepsilon_d = 0.08h$ and $\varepsilon_d = 0.8h$; the most accurate and stable results are obtained with $\varepsilon_d = 0.8h$ because the error decreases and then from a value of Δt sufficiently small the curve remains flat as Δt decreases, this behavior does not occur with the error curve of $\varepsilon_d = 0.08h$ that undergoes a slight increase as Δt becomes smaller and smaller. In Figure 2 we see that the solutions remain stable because the integrals are calculated with high accuracy (order 10); however, here too, it is noticeable the existence of a threshold value of Δt below which the solutions for the conventional LG method and the subgrid viscosity LG method with $\varepsilon_d = 0.0008h$ lose stability because the error curves grow slowly as Δt decreases. As in Figure 1, the most accurate and stable solution is the one obtained with $\varepsilon_d = 0.8h$. We must say that the flat region of the error curves in these figures for $\varepsilon_d = 0.8h$ and $\varepsilon_d = 0.08h$ is due to the fact that when Δt is sufficiently small the temporal component of the error is negligible as compared with the spatial error. The same results as those in Figure 2 are obtained if we employ a quadrature rule of order 14.

Finally, from the evidences of these numerical experiments we can conclude that the subgrid viscosity LG method with $\varepsilon_d \simeq h$ is more stable and accurate than the conventional LG method for convection-diffusion-reaction problems at high Péclet numbers.

References

[1] A. Bermúdez, M. R. Nogueiras and C. Vázquez, Numerical analysis of convection-diffusion-reaction problems with higher order characteristics/finite elements. Part II: Fully discretized schemes and quadratuire formulas. SIAM J. Numer. Anal., 44:1854-1876, 2006.

[2] R. Bermejo, P. Galán del Sastre and L. Saavedra, A second order in time modified Lagrange-Galerkin finite element method for the incompressible Navier-Stokes equations. SIAM J. Numer. Anal., to appear, 2012.

[3] R. Bermejo and L. Saavedra, Modified Lagrange-Galerkin methods of first and second order in time for convection-diffusion problem. Numer. Math., 120: 601-638, 2012..

[4] R. Bermejo, Analysis of a class of quasi-monotone and conservative semi-Lagrangian advection schemes. Numer. Math., 87: 597-623, 2001.

[5] K. Boukir, Y. Maday, B. Métivet and E. Razanfindrakoto, A high-order characteristics/finite element method for the incompressible Navier-Stokes equations. International J. Numer. Methods Fluids., 25: 1421-1454, 1997.

[6] A. N. Brooks and T. J. R. Hughes, Streamline upwind/Petrov-Galerkin formulations for convection dominated flows with particular emphasis on the incompressible Navier-Stokes equations. Comput. Meth. Appl. Mech. Engrg., 32: 199-259, 1982.

[7] E. Burman and P. Hansbo, Edge stabilization for the Galerkin approximations of convection-diffusion-reaction problems. Comput. Methods Appl. Mech. Engrg., 193: 1437-1453, 2004.

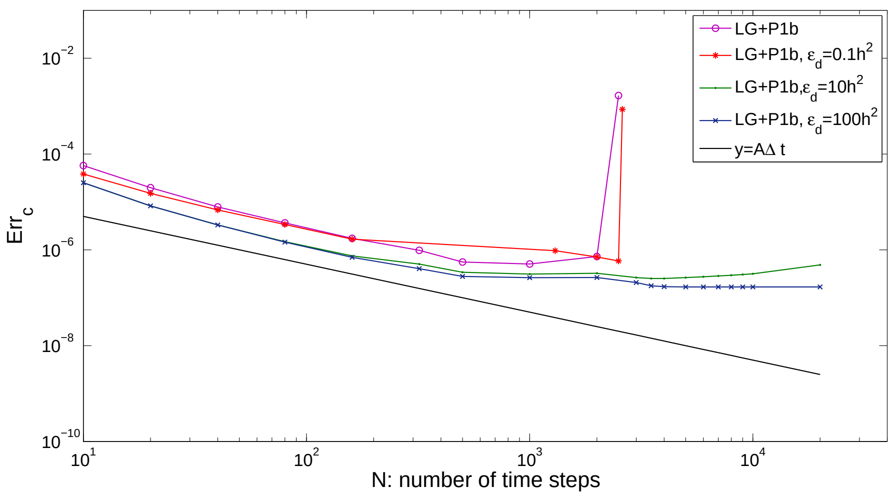

FIGURE 1. Error obtained with different time steps using the finest mesh $h = 1/128$ and with the quadrature rule of order 5

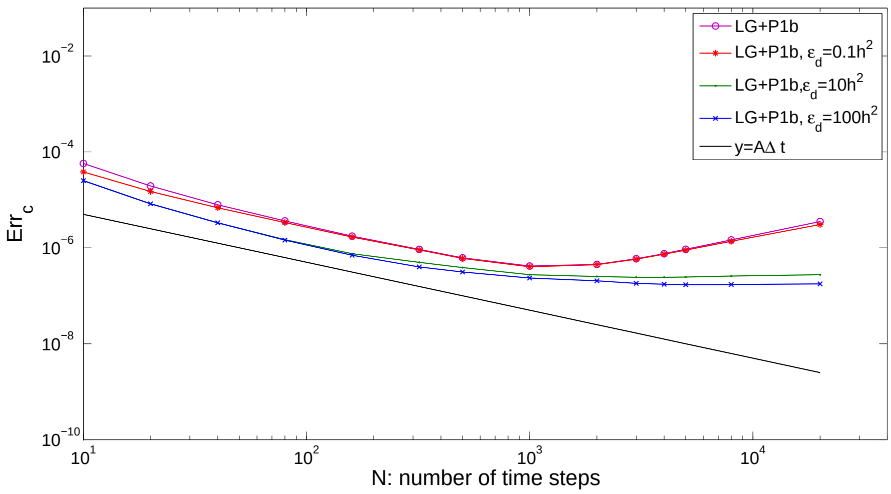

FIGURE 2. Error obtained with different time steps using the finest mesh $h = 1/128$ and with the quadrature rule of order 10

[8] M.A. Celia, T.F. Russell, I. Herrera and R.E. Ewing, An Eulerian-Lagrangian localized adjoint method for the advection-diffusion equations. Adv. Water. Resources, 13: 187-206, 1990.
[9] J. Douglas and T.F. Russell, Numerical methods for convection-dominated diffusion problems based on combining the method of characteristics with finite element or finite difference procedures. SIAM J. Numer. Anal., 19: 871-885, 1982.
[10] M. Falcone and R. Ferreti, Convergence analysis for a class of high-order semi-Lagrangian advection schemes. SIAM J. Numer. Anal., 35: 909-940, 1998.
[11] J.L. Guermond, Stabilization of Galerkin approximations of transport equations by subgrid modelling. M2AN Math. Model. Numer. Anal., 33: 1293-1316, 1999.
[12] P. Hansbo, The characteristic streamline diffusion method for convection-diffusion problems. Comput. Meth. Appl. Mech. Engrg. 96: 239-253, 1992.

[13] P. Hansbo, The characteristic streamline diffusion method for time-dependent incompressible Navier-Stokes equations. Comput. Meth. Appl. Mech. Engrg., 99: 171-186, 1992.
[14] P. Hartman, Ordinary Differential Equations, Wiley, New York, 1973.
[15] J.G. Heywood and R. Rannacher, Finite element approximations of the nonstationary Navier-Stokes problem part IV: error analysis for second-order time discretization, SIAM J. Numer. Anal., 27: 353-384, 1990.
[16] T.J.R. Hughes, Multiscale phenomena, Green's functions, the Dirichlet-to-Neumann formulation, sub-grid scale models, bubbles and the origin of stabilized methods. Comput. Methods Appl. Mech. Engrg., 127: 387-401, 1995.
[17] T. J. R. Hughes. L.P. Franca and G.M. Hulbert, A new finite element formulation for computational fluid dynamics. VIII. The Galerkin/least-squares method for advection-diffusive equations. Comput. Meth. Appl. Mech. Engrg., 73: 173-189, 1989.
[18] C. Johnson, A new approach to algorithms for convection problems which are based on exact transport + projection. Comput. Meth. Appl. Mech. Engrg., 100: 45-62, 1992
[19] V. John, S. Kaya and W. Layton, A two-level variational multiscale method for convection-dominated convection-diffusion equations. Comput. Methods. Appl. Mech. Engrg., 195: 4594-4603, 2006.
[20] W. Layton, A connection between subgrid scale eddy viscosity and mixed methods. Appl. Math. Comp., 133: 147-157, 2002.
[21] K.W. Morton, Numerical Solution of Convection diffusion Problems, Chapman and Hall, London, 1996.
[22] K. W. Morton, A. Priestley and E. Süli, Stability of the Lagrange-Galerkin method with non-exact integration. M2AN Math. Model. Numer. Anal., 22: 625-653, 1988.
[23] O. Pironneau, On the transport-diffusion algorithm and its applications to the Navier-Stokes equations. Numer. Math., 38: 309-332, 1982.
[24] L. Song, Y. Hou and H. Zheng, A variational multiscale method based on bubble functions for convection-dominated convection-diffusion equations. Appl. Math. and Comput., 217: 2226-2237, 2010.
[25] E. Süli, Convergence and nonlinear stability of the Lagrange-Galerkin method for the Navier-Stokes equations. Numer. Math., 54: 459-483, 1988.
[26] H. Wang, H.K. Dahle, R. E. Ewing, M.S. Espedal, R.C. Sharpley and S. Man, An ELLAM scheme for advection-diffusion equations in two-dimensions. SIAM J. Sci. Comput., 20: 2160-2194, 1999.

Departamento de Matemática Aplicada ETSII, Universidad Politécnica de Madrid, José Gutérrez Abascal, 2 28006 Madrid, Spain
E-mail: `rbermejo@etsii.upm.es`

Departamento de Matemática Aplicada ETSA, Universidad Politécnica de Madrid, Avda. Juan de Herrera, 2 28040 Madrid, Spain
E-mail: `pedro.galan@upm.es`

Departamento de Fundamentos Matemáticos ETSIA, Universidad Politécnica de Madrid, Plaza del Cardenal Cisneros, 2 28040 Madrid, Spain
E-mail: `laura.saavedra@upm.es`